OPTIMIZED DESIGN AND TESTING OF A PROTOTYPE MILITARY BRIDGE SYSTEM FOR RAPID IN-THEATER CONSTRUCTION

Joseph P. Hanus, PE
Lieutenant Colonel, US Army
University of Wisconsin at Madison
Madison, WI 53706

Lawrence C. Bank, PhD, PE
Professor, Civil Engineering Department
University of Wisconsin at Madison
Madison, WI 53706

James C. Ray, PE
Research Structural Engineer
Engineer Research and Development Center
Vicksburg, MS 39180

Gerardo I. Velazquez, PE
Research Structural Engineer
Engineer Research and Development Center
Vicksburg, MS 39180

ABSTRACT

A prototype military bridge system using in-theater concrete with a deployable, folding truss support, and stay-in-place-form system was designed and tested. The bridge's primary advantage is a reduction in deployment requirements because of the use of in-theater materials. Numerical optimization was used in the design to reduce the deployable component weights. The results showed a potential 50% weight savings compared to the US Army Rapidly Emplaced Bridge. An experimental program investigated the critical deck component capacity, and physical and statistical analysis confirmed the deck has a military load class 70 axle load capacity.

1. INTRODUCTION

The US Army Future Force doctrine requires rapidly deployable forces with minimal logistical requirements. The current US military bridging systems are logistically burdensome because they require the deployment of a complete bridge, i.e., all components must deploy from out-of-theater storage sites to in-theater construction sites. An innovative approach to solving this problem is necessary to reduce bridging logistical requirements. This paper will outline the development of an innovative bridge with both deployable and in-theater constructed components. The design parameters, component selection, and design basis using numerical optimization to achieve the minimal component deployment weight are discussed. The physical and statistical analysis of the test results on the system's critical component confirm it's crossing capacity.

The bridge's development extended from a recently completed bridging system study for the US Army Future Combat System (Bank et al., 2005). In that study a wide range of concepts were systematically investigated and analyzed. Innovative materials, components, and systems were studied over a two year research program. A multi-disciplinary approach to the selection and evaluation process ensured the best concepts were selected for further development (Bank et al., 2005). The concept selected and outlined in this paper involves folding bridge components that are expandable from a transportation configuration into a construction and operational configuration. Although the concept is closely related to some current military bridging systems, the innovative value is in the component details. The concept is shown in general in Figure 1. In Stage 1, the components are deployed to the theater of operations in a folded and/or nested configuration. In Stage 2, the support truss components are expanded, and in Stage 3 the stay-in-place form and reinforcement components are attached. Finally, in Stage 4, a cast-in-place deck with in-theater concrete completes the bridge. A unique feature of the final bridge is that the truss top chord is also the deck for vehicles crossing. This critical component is the primary focus of the results presented in this paper.

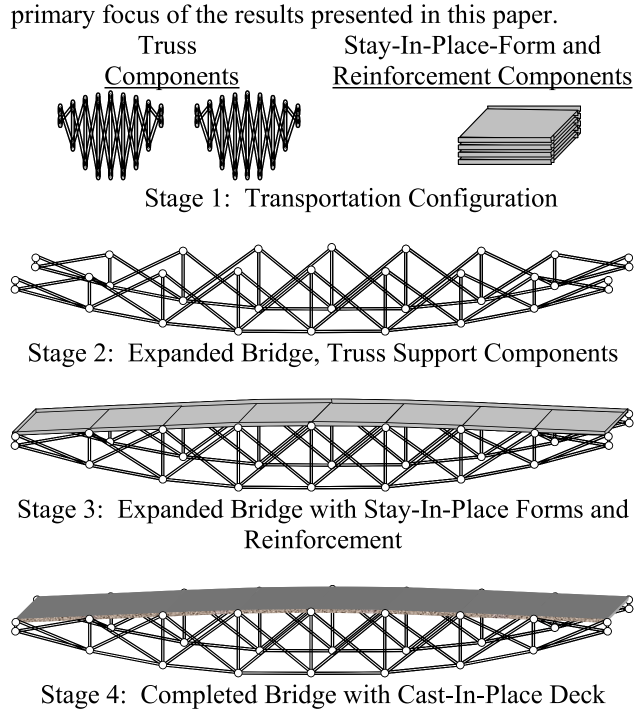

Fig. 1. Concept Construction Sequence

Report Documentation Page

Form Approved
OMB No. 0704-0188

1. REPORT DATE **01 NOV 2006**	2. REPORT TYPE **N/A**	3. DATES COVERED **-**

4. TITLE AND SUBTITLE **Optimized Design And Testing Of A Prototype Military Bridge System For Rapid In-Theater Construction**	5a. CONTRACT NUMBER 5b. GRANT NUMBER 5c. PROGRAM ELEMENT NUMBER
6. AUTHOR(S)	5d. PROJECT NUMBER 5e. TASK NUMBER 5f. WORK UNIT NUMBER
7. PERFORMING ORGANIZATION NAME(S) AND ADDRESS(ES) **University of Wisconsin at Madison Madison, WI 53706**	8. PERFORMING ORGANIZATION REPORT NUMBER
9. SPONSORING/MONITORING AGENCY NAME(S) AND ADDRESS(ES)	10. SPONSOR/MONITOR’S ACRONYM(S) 11. SPONSOR/MONITOR’S REPORT NUMBER(S)

12. DISTRIBUTION/AVAILABILITY STATEMENT
Approved for public release, distribution unlimited

13. SUPPLEMENTARY NOTES
See also ADM002075., The original document contains color images.

14. ABSTRACT

15. SUBJECT TERMS

16. SECURITY CLASSIFICATION OF:			17. LIMITATION OF ABSTRACT	18. NUMBER OF PAGES	19a. NAME OF RESPONSIBLE PERSON
a. REPORT **unclassified**	b. ABSTRACT **unclassified**	c. THIS PAGE **unclassified**	**UU**	**8**	

Standard Form 298 (Rev. 8-98)
Prescribed by ANSI Std Z39-18

2. BRIDGE DESIGN

2.1 Design Parameters

The bridge was designed for Military Load Class (MLC) 30, which is the assumed classification for the US Army Future Combat System (Boeing, 2006). However, the design was checked with respect to overloading for an M1 tank, i.e., MLC 70. The bridge was designed to span 48 feet, which is based upon current US Army temporary bridging systems, i.e., the Wolverine and Rapidly Emplaced Bridge Systems (Connors et al., 2006-2007). The intent is for the new bridge to replace these current systems as a semi-permanent to permanent bridge. Additionally, the predominate length of bridge gaps in potential theater of operations includes 48-ft spans, according to a 2003 Bridge Study by the US Army Maneuver Support Center, Fort Leonard Wood, Missouri.

The design and analysis focused on a single treadway, which carries half the required load. Two treadways is the simplest configuration (Fig. 2) or a full-width system is possible with three parallel treadways (Fig. 3).

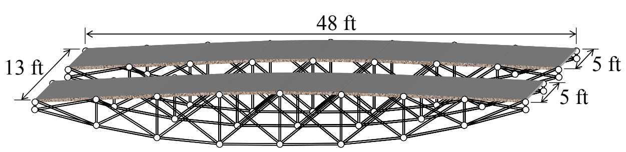

Fig. 2. Treadway System

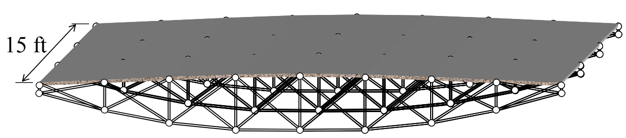

Fig. 3. Full Width System

2.2. Component Selection

The two primary components in the bridge are the support and the deck components. Several different materials and sub-components were considered, and the selection process considered strength to weight ratios and immediate application for testing, i.e., commercially available materials and sub-components were preferred.

The support component, consisting of the structural elements below the deck, was configured as a truss with the ability to fold for deployment and expand for construction. The primary focus was on the strength and stiffness of this component during construction and operation of the bridge. The support component was designed with 7005 T53 aluminum, which is commonly used in military bridging. Hollow circular tube sections were selected to reduce the component weight while maintaining sufficient buckling resistance.

The deck component consists of the structural elements above the support component. This component includes deployed and in-theater materials. The stay-in-place form and reinforcement sub-component was designed with pultruded glass fiber-reinforced-polymer material that included plates and structural shapes for longitudinal and transverse stiffness. This material represents the state-of-art for light-weight bridging material. A commercially available sub-system, the GridForm System by Strongwell, was selected. This system had been successfully tested as a stay-in-place form and reinforcement system at the University of Wisconsin-Madison for use in Federal Highway Administration Innovative Bridge Research and Construction projects (Bank et al., 2006; Berg et al., 2006; Ringelstetter et al., 2006). A specific GridForm system was selected for its stiffness and strength characteristics. The selected system consisted of longitudinal 2-inch T-bars, with ½ inch diameter transverse bars, epoxied to a 1/8th inch plate. The longitudinal T-bar spacing was determined using numerical optimization while the transverse bar spacing was set at 4 inches based upon successful testing of similar systems.

Concrete procured in-theater would be cast into the stay-in-place-form and reinforcement system. The concrete was assumed to be a standard 4,000 psi compressive strength mix with no additives. The US Army Mobile Concrete Mixer was the assumed transport and mixing vehicle with a material capacity of 8 cubic yards (Fig. 4) (United States. Dept. of the Army., 1979).

Fig. 4. US Army Mobile Concrete Mixer

2.3 Design Basis

The design basis was a composite of the US Army and civilian design codes. The US Army's Military Nonstandard Fixed Bridging Field Manual was used to determine the required loadings for MLC 30, which included a single axle load, multiple axle loads, and a tank uniform load (United States. Dept. of the Army., 2002). This manual also identified load factors for live and dead load (1.7 and 1.4, respectively), a dynamic load allowance (15%), and the effective width for concrete decks (4ft + 0.06 L_{span}). The US Army's Trilateral Design and Test Code (TDTC) for Military Bridging and Gap-Cross Equipment was used to identify the material factors for the aluminum components (0.75 for yielding and 0.67 for

buckling) and the minimum treadway width of 5 feet for MLC 30 bridges (United States. Dept. of the Army., 1996). The Aluminum Association Design Manual was used to establish the strength limit state equations for the aluminum components (tensile and compression) (Aluminum Association., 2005). The American Concrete Institute's "Guide for the Design and Construction of Structural Concrete Reinforced with FRP Bars was used to establish the material factors (0.65 for over-reinforced flexure and 0.75 for shear) and strength limit state equations (flexure, flexural shear, and punching shear) for the FRP deck components " (American Concrete Institute., 2006).

3. NUMERICAL OPTIMIZATION

3.1 Objective and Trade-Off Decisions

The optimization objective was to minimize the weight of the deployable components, i.e., support components, and stay-in-place-form and reinforcement components. A wide range of optimization techniques were considered, e.g., discrete vs. continuous, geometric vs. material, etc. However, the trade-off of rigorous theoretical optimization for practical application was required to advance the concept to experimental testing.

The structural optimization analysis focused on a linear elastic analysis in the critical structural state with a cracked deck. This state assumed that the continuous cast deck was cracked at the truss nodes such that each deck component spanned between truss nodes in a pin-pin support configuration. The transition between the continuous deck and pin-pin deck would redistribute forces from the deck into the truss and shift negative end moment magnitudes to the center of deck spans. Hence, the pin-pin support configuration resulted in the largest truss forces and greatest center of deck span moments.

The truss panel spans in the support component were set at discrete values of 48, 72, and 96 inches. The selection of these span lengths was based upon currently available stay-in-place-form systems. The cast-in-place deck depth range was from 4.25 to 10.25 inches. The 4.25 inch bound was based on minimal structural capacity. The 10.25 inches represented the capacity of two Mobile Concrete Mixers (United States. Dept. of the Army., 1979) for two treadways. Each mixer has the capacity to cast two 5.125 inches treadway decks.

The bridge system optimization was decomposed into the two components for analysis and results combined for a total treadway system weight. The decomposition simplified the numerical optimization and provided insight into the individual component behavior which would have been masked in a single optimization model.

3.2 Support Component Optimization

The support component was optimized as a non-linear constrained problem (Haftka et al., 1992). The objective was to minimize the deployment weight, which was a function of the members' cross-sectional area and lengths. The variables include the truss panel spans (48, 72, and 96 inches), the deck depth (4.25 to 10.25 inches), member cross-sectional areas and node locations. The vertical locations of truss nodes varied continuously in the optimization model. The upper chord nodes were limited by a maximum deck slope of 3% and the lower chord nodes were limited by a minimum gap depth of 48 inches.

The constraints in the support component optimization were in accordance with the design basis and included deflection and strength limit states. The deflection limit was span/100, which was 5.76 inches. The strength limit states included tension and compression with appropriate reductions to prevent member buckling. The deck compression limit in the truss model was $f'_c/10$. This constraint limited the deck compression stress to ensure sufficient capacity to act primarily as a flexural member in the deck component optimization. The member cross-sectional areas were related to the radius of gyration based upon commonly available sections and a 10:1 ratio of diameter to wall thickness.

The required loadings for MLC 30 were applied to the system with multiple load cases for each axle, truck, and track loading. The load cases were applied sequentially to upper truss nodes, which simulated vehicles crossing the bridge. Hence, the number of constraints was multiplied by the number of load cases. For example, for the 48 inch truss panel system there were 111 constraints for each of the 45 load cases, which resulted in 4,995 constraints in the optimization model.

A MATLAB program was written with the *fmincon* function to find the local minima within the design space. This function uses a Sequential Quadratic Programming (SQP) based optimization method with a Broyden-Fletcher-Goldfarb-Shanno (BFGS) algorithm for the Hessian estimation (MathWorks, 2006). The optimization results are shown in Figure 5 as continuous functions for each truss panel length with respect to a deck depth. There is a set of member cross-sectional areas and node locations for each discrete point on the functions.

As shown in Figure 5, the support component behavior indicated local minima at the deck depths of 6.40, 5.84, and 5.79 inches for the truss panel lengths 48, 72, and 96 inches, respectively. The associated support component weights for each of these minima were 538, 496, and 475 lbs, respectively. These values represent the ideal weight for the support component for a single

treadway. With each weight there is an associated set of cross-sectional areas and nodes, for the minimum deck depth for a particular truss panel length.

3.3 Deck Component Optimization

The deck component was also optimized as a non-linear constrained problem (Haftka et al., 1992). The objective was to minimize the deployment weight, which was a function of the reinforcement spacing and stay-in-place-form depth. The variables include the truss panel spans (48, 72, and 96 inches), the deck depth (4.25 to 10.25 inches), and spacing of the longitudinal T-Bars. The spacing variable was bound by the manufacturer's limits of 1.2 to 12 inches. Multiple fabrication jig combinations were available and the spacing variable was left continuous between the limits with further refinement possible later in the analysis.

The constraints in the deck component optimization were in accordance with the design basis and included deflection and strength limit states. The construction deflection limit was span/180, the live load deflection limit was span/100, and the strength limit states included flexural, flexural-shear, and punching shear. The single axle load was the most critical MLC 30 loading and it was applied at the center of the deck span between simple supports in the optimization model.

A second MATLAB program with *fmincon* was written to run the deck optimization model (MathWorks, 2006). The results of the optimization are shown in Figure 6 as continuous functions for each truss panel length with respect to the deck depth. There is a T-bar spacing for each discrete point on the functions. Note – the deck component weight includes only the elements which deploy, not the cast-in-place in-theater concrete.

The optimization did not find local minima within the deck depth range of 4.25 to 10.25 inches. However, the behavior indicates the functions are approaching local minima beyond a deck depth of 10.25 inches.

3.4 Combined Component Optimization

The combined support and deck component optimization results are shown in Figure 7. The minimum total system weight, across all the variables, was 1,310 lbs. The associated variable values were a truss panel span of 72 inches, a deck depth of 9 inches, and a T-bar spacing of 7.48 inches. Additionally, there was a set of support system cross-sectional areas and node locations with this minimum weight. However, further consideration was given to these results with respect to a practical implication. The depth of 9 inches requires two Mobile Concrete Mixers. The maximum deck depth for one Mobile Concrete Mixer is 5.125 inches. The minimum weight at 5.125 inch deck depth was 1,432 lbs, with a truss panel span of 72 inches and T-bar spacing of 3.00 inches. It was preferred to limit the number of mixers to one and sacrifice 122 lbs in total weight.

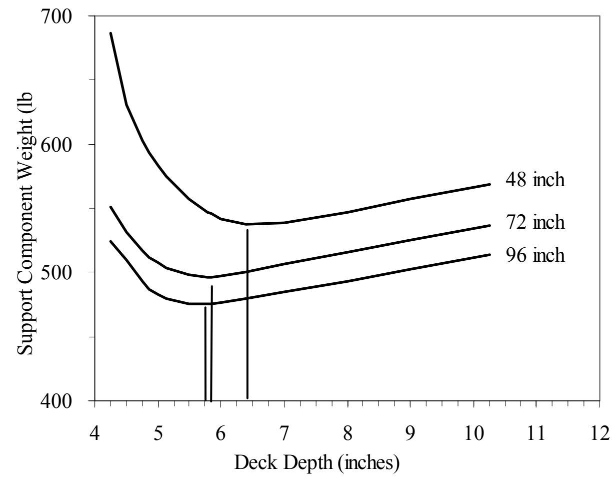

Fig. 5. Support Component Optimization Results

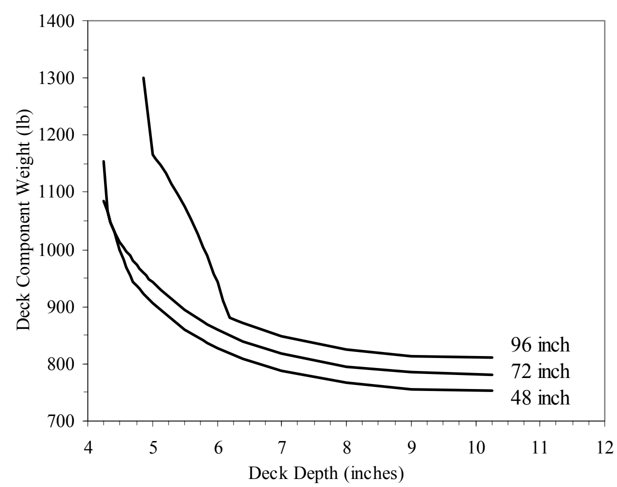

Fig. 6. Deck Component Optimization Results

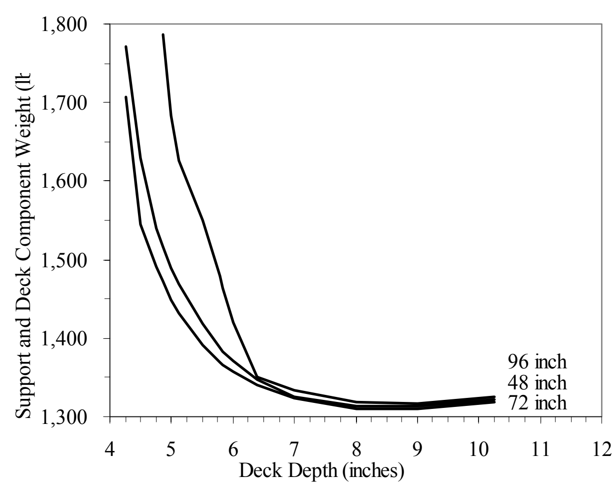

Fig. 7 Combined Optimization Results

4. EXPERIMENTAL PROGRAM

The critical component in the bridge was the deck because it is a non-traditional component in terms of material and structural application. It was fabricated with state-of-the-art pultruded glass fiber-reinforced-polymer material, and in the bridge it acts as the deck and top chord of the truss. Hence, it was the focus of the initial experimental program to investigate the bridge feasibility.

4.1 Objectives

The experimental program's primary objective was to confirm the capacity of the optimized deck component. The testing was designed to investigate two primary variables in a replicated two-level factorial experiment. The variables in the investigation were axial load application and the addition of synthetic fibers to the cast-in-place concrete deck. The axial load application was chosen as a variable because the design basis did not explicitly address this member type. The compression stress in the deck was limited in the numerical optimization such that the flexural condition would dominate in the design. However, the effect of the axial load was not specifically included in the deck component optimization process. Hence, testing for its effect was important to understanding the deck component behavior. The addition of fibers to the concrete was also included because of the potential benefits. These fibers are commonly added to concrete for durability, crack control, and early strength development. However, their effect on the deck component strength was not known; hence, inclusion in the testing was needed. Both testing variables represented design elements that were not accounted for explicitly in the numerical optimization models because their effects were unknown. Such variables were ideal for the experimental program.

4.2 Experiments

The deck specimens in the experiments were based upon the numerical optimization results. The specimens were 5 feet wide, 5.125 inches deep, and spanned 72 inches. The stay-in-place form and reinforcement system included longitudinal 2-inch T-bars spaced at 3 inches with transverse ½ inch diameter rods spaced at 4 inches. A 1/8-inch plate was epoxied to the bottom to act as the specimen's form-work (Fig. 8). The specimens were constructed on simple supports that spanned 72 inches (Fig. 9), which simulated the in-field deck component casting on the support components.

The nominal concrete compressive strength was 4,000 psi as it was in the numerical optimization model. A blended polypropylene fiber material was added at 5 lb per cubic yard to 4 of the 8 specimens for the fiber-reinforced-concrete (FRC).

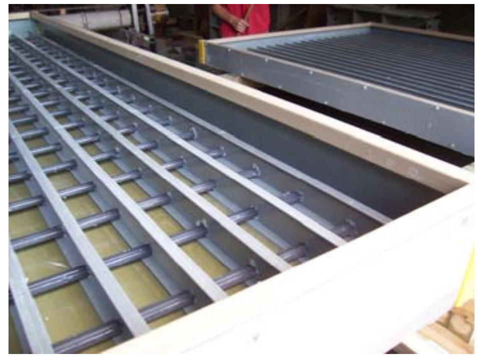

Fig. 8. Stay-In-Place Form and Reinforcement

Fig. 9. Stay-In-Place Forms Prepared to Cast Decks

The specimens were tested with transverse loading that represented the MLC 30 axle load and tire pressure area. The specimens were then loaded until failure. Half of the specimens also included an axial load in accordance with the numerical optimization model:

$$A = 0.85T + 14.5 \text{ (kips)} \tag{1}$$

where A = applied axially load (kips),
T = applied transverse load (kips).

Figure 10 shows a specimen in the transverse only load frame and Figure 11 shows a specimen in the transverse and axial load frame. The transverse load was applied with a 200 kip hydraulic actuator and the axial load was applied with two 120 kip hydraulic jacks in a horizontal internally constrained load frame. The horizontal frame was designed to ensure the end rotations were free such that the results could be compared to the transverse only loaded specimens without end constraint effects. Both load frames represented simply supported deck components that would develop once negative moment cracking would occur above the truss panel points. It was assumed that such cracking would eventually occur in the system and the critical deck structural loading would occur in the simple supported configuration between truss panel nodes.

Fig. 10. Transverse Only Loaded Specimen

Fig. 11. Transverse and Axially Loaded Specimen

Strain gages and displacement instrumentation were attached to the specimen to record the behavior and confirm consistent testing protocol. The specimens were constructed and tested in a random order to facilitate statistical analysis with an assumed experimental error normal distribution about zero.

The eight specimens failed in a similar manner with flexural failure due to concrete crushing along the center of slab span. The failure was identified with center span cracking and associated concrete strains beyond the design value of 0.003. The ultimate loads, concrete strain at ultimate, and concrete strength are shown in Table 1.

4.3 Physical Analysis of the Results

The specimens exceeded the required axle load for MLC 30, i.e., 13.5 kips. The over capacity was due to the optimization design basis equations and assumptions. The specimen failure mode was flexural with concrete crushing. The concrete crushing was the result of the over-reinforced section, which was predicted in the flexural design basis equation. However, the controlling design equation was flexural shear followed by punching shear and then flexure. Hence, because the test specimens surpassed the flexural and punching shear design basis, they developed the larger flexural capacity. Additionally, the concrete strain at failure was an average of 4400×10^{-6}, which is greater than the 3000×10^{-6} used in the flexural design basis equation. Also, the nominal concrete strength used in the flexural design basis equation was 4,000 psi; whereas the average strength was 5,410 psi. Hence, the effect of these design factors and assumptions contributed to the specimens' over-strength.

The load versus deflection graphs for the tests are shown in Figure 12. The specimens had an average deflection at ultimate load of 1.22 inches, which correlates to a span/60 for the 72 inch specimens. However, at the MLC 30 (13.5 kips) the average deflection was 0.086 inches or span/837, and at MLC 70 (25.5 kips) the average deflection was 0.176 inches or span/409. Both values meet the design requirements.

Table 1. Test Results

#	Axial Load	FRC	Ultimate Load (kips)	Concrete Strain at Ultimate ($\times 10^{-6}$)	Concrete Strength (psi)
1	Yes	No	83.2	4460	4910
2	Yes	No	90.1	4320	5160
3	Yes	Yes	80.6	3720	5530
4	Yes	Yes	81.2	4780	5930
5	No	No	96.8	3860	5130
6	No	No	90.9	3990	5160
7	No	Yes	98.0	4300	5620
8	No	Yes	89.6	5780	5860
		Average	88.0	4400	5410

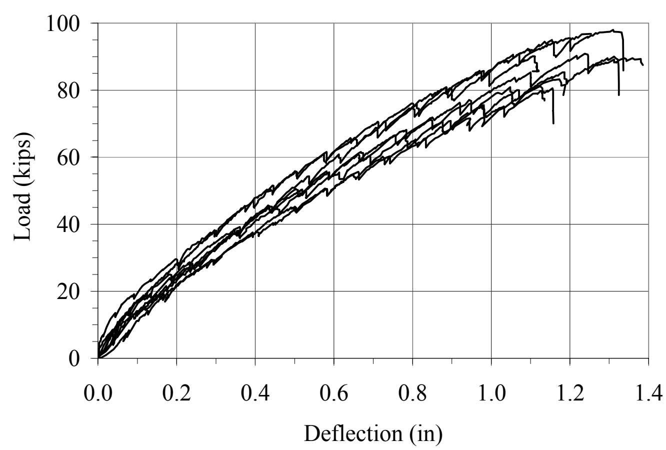

Fig. 12. Deflection versus Load

The overall behavior of the specimens was nearly linear to failure. This type of non-ductile failure is not preferred, but is inevitable in over-reinforced FRP sections. The inherent safety factor of ductile members is replaced with larger factors of safety in such sections (Bank, 2006).

4.4 Statistical Analysis of the Results

Statistical analysis of the results provided a qualitative confidence level to drawing conclusions with respect to the effects of the experiment variables and their effect on specific yields. In this test, the axial load and fiber reinforced concrete effects were analyzed with respect to the ultimate load. The ultimate load is the primary concern with the deck component design. The analysis procedure was in accordance with design of experiments techniques (Box et al., 1978). The confidence interval to test significance was based upon a Studentized M-Test alpha of 10% as follows:

$$(100-\alpha)CI = Effect \pm M(SE) \qquad (2)$$

where M = Studentized M-Test Value, 2.98,
SE = standard error, 3.096 based upon a pooled variance,
CI = confidence interval, 90%.

The test variables were determined to be significant if their effect was beyond the confidence interval calculation in Eq (2), i.e., 2.98(3.096) = 9.225. The two variables and their combined effects are shown in Table 2 with the results of the significance tests.

Table 2. Significance Test

Term	Effect	Significance Test
Axial Force	-10.050	Yes
Fiber Reinforced Concrete (FRC)	-2.900	No
Combined Effect of Axial Force and FRC	-2.850	No

Based upon the results only the axial force had a significant effect on the ultimate load. The fitted model with the grand mean and coefficient for the axial load effect was established as follows:

$$y_{ij} = 88.0 \pm 5.025x_1 + \varepsilon_{ij} \qquad (3)$$

where x_1 = binary value of +1 without axial load and -1 with axial load,
$\varepsilon_{ij} \sim$ error assumed IIDN$(0,\sigma^2)$.

Estimated fitted values for each test and associated residuals were calculated. The residuals represented the difference between the actual test and the fitted model. The results are shown in Table 3.

Table 3. Test Results

Specimen		Ultimate Load		
#	Axial Load	Actual (kips)	Fitted Model	Residuals
1	Yes	83.2	83.775	-0.575
2	Yes	90.1	83.775	6.325
3	Yes	80.6	83.775	-3.175
4	Yes	81.2	83.775	-2.575
5	No	96.8	93.825	2.975
6	No	90.9	93.825	-2.925
7	No	98.0	93.825	4.175
8	No	89.6	93.825	-4.225

The error assumption of IIDN$((0,\sigma^2)$. i.e., independently tests, identically tested, and distributed normally, was checked. The residual normal plot (Fig. 13) and the plot of the residuals with respect to test order (Fig. 14) were used in validating the error assumption. The assumption was accepted because residual values were normally distributed and did not display any patterns with respect to run order.

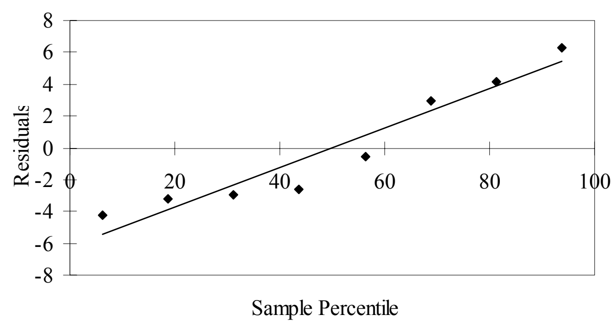

Fig. 13. Normal Plot of Residual Values

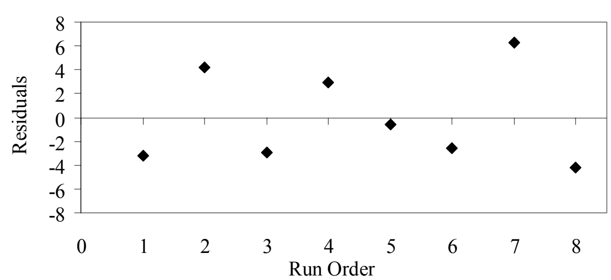

Fig. 14. Residuals versus Run Order

4.5 Integrated Physical and Statistical Analysis

Based upon the statistical results, the four specimens with axial load should be considered for establishing an assured capacity for the optimized deck component. The average and standard deviation of the four specimens with axial load were 83.8 and 4.36 kips, respectively. These four specimens included two with FRC and two without FRC. However, as statistically proved, the FRC did not significantly affect the specimen's ultimate load.

5. CONCLUSIONS

Several conclusions can be made from the numerical optimization and experimental program results for the innovative bridging system presented herein. The numerical optimization results indicate that significant weight savings can be achieved with this concept as a semi-permanent bridge. The US Army Rapidly Emplaced Bridge System (REBS) weighs nearly 11,000 lb (United States. Dept. of the Army., 2006). The numerical optimization results indicate a single deployable treadway could weigh less than 1,500 lbs. Although this is an ideal optimized weight, a reasonable assumption could be made that a full system, i.e., two treadways, with fully designed lateral support and connection details could weigh less than half of the REBS bridge system. As a result, when assault bridging systems are removed from gap crossing sites, two of the new bridges could be deployed for use as a semi-permanent bridge for the weight of one REBS. The physical and statistical analysis of the experimental results establishes the assured capacity of the optimized deck component at 75.1 kips (mean minus two standard deviations). This capacity provides an overall safety factor of 5.6 and 2.9 for MLC 30 and 70, respectively.

The presented bridge requires additional analysis and testing, which is planned. Multiple deck component behavior, i.e. cracking across the truss nodes, and the connections between the deck and support components must be investigated. Additionally, the support component deployability must also be investigated. The results of these investigations and the results presented herein establish the significant potential of this bridge concept. Successful development of this innovative military bridge system will support the US Army Future Force doctrine and provide mobility support to US Army Future Combat System in future theaters of operation.

ACKNOWLEDGEMENTS

The work reported herein was an extension of the US Army Battlespace Gap Defeat Project (Bank et al., 2005). FRP material was donated by Strongwell and concrete fiber reinforcement was donated by Propex Concrete Systems. The axial load frame was fabricated by Palmer Manufacturing with Enerpac hydraulic load equipment. The work was performed in the Structures Testing and Materials Lab at the University of Wisconsin – Madison. Permission to publish was granted by Director, Geotechnical & Structures Laboratory, US Army COE.

REFERENCES

Aluminum Association., 2005: *Aluminum Design Manual: Specifications & Guidelines for Aluminum Structures*. Aluminum Association, 568 pp.

American Concrete Institute., 2006: *Guide for the Design and Construction of Structural Concrete Reinforced with FRP Bars*. *ACI; 440.1R-06*, American Concrete Institute, 44 pp.

Bank, L. C., 2006: *Composites for Construction: Structural design with FRP materials*. John Wiley & Sons, 551 pp.

Bank, L. C., J. S. Russell, J. P. Hanus, J. C. Ray, and G. I. Velaquez, 2005: Conceptual Studies for Rapidly Deployable Battlespace Gap Structures. W912H2-04-P-0150, 182 pp.

Bank, L. C., M. G. Oliva, J. S. Russell, D. A. Jacobson, M. Conachen, B. Nelson, and D. McMonigal, 2006: Double Layer Prefabricated FRP Grids for Rapid Bridge Deck Construction: Case Study. *ASCE Journal of Composites for Construction*, **10,** 201-121.

Berg, A. C., L. C. Bank, M. G. Oliva, and J. S. Russell, 2006: Construction and Cost Analysis of an FRP Reinforced Concrete Bridge Deck. *Construction and Building Materials*, **20,** 515-526.

Boeing: 2006 FCS Briefing Book. [Available online from www.boeing.com/defense-space/ic/fcs.html.]

Box, G. E., J. S. Hunter, and W. G. Hunter, 1978: *Statistics for Experimenters: An introduction to design, data analysis, and model building*. Wiley, 653 pp.

Connors, S. C. and C. F. Foss, Eds., 2006-2007: *Jane's Military Vehicles and Logistics*. 27th ed. Jane's Information Group, 1098 pp.

Haftka, R. T. and Z. Gürdal, 1992: *Elements of Structural Optimization*. 3rd ed. *Solid mechanics and its applications*, Kluwer Academic Publishers, 481 pp.

MathWorks, 2006: *Optimization Toolbox, for use with MATLAB*. The MathWorks, 478 pp.

Ringelstetter, T. E., L. C. Bank, M. G. Oliva, J. S. Russell, F. Matta, and A. Nanni, 2006: Development of Cost-Effective Structural FRP Stay-in-Place Formwork System for Accelerated and Durable Bridge Deck Construction. *Transportation Research Record*, Washington, DC, National Research Council, 16 pp.

United States. Dept. of the Army., 1979: *Technical Manual 5-3895-372-10 for Concrete Mobile Mixer*. Headquarters, Dept. of the Army, 176 pp.

——, 1996: *Trilateral Design and Test Code for Military Bridges and Gap-Crossing Equipment*. US Army Tank-Automotive and Armaments Command, 118 pp.

——, 2002: *Field Manual 3-34.343 for Military Nonstandard Fixed Bridging*. Headquarters, Dept. of the Army, 552 pp.

——, 2006: *Technical Manual 5-5420-280-23&P for Rapidly Emplaced Bridge*. Headquarters, Dept. of the Army, 956 pp.